

From Hindbrain Segmentation to Breathing After Birth

Developmental Patterning in Rhombomeres 3 and 4

**Fabrice Chatonnet,¹ Eduardo Domínguez del Toro,²
Muriel Thoby-Brisson,¹ Jean Champagnat,¹ Gilles Fortin,¹
Filippo M. Rijli,³ and Christelle Thaëron-Antôno*,¹**

¹UPR 2216 Neurobiologie Génétique et Intégrative, Institut de Neurobiologie Alfred Fessard, CNRS, 1, av. de la Terrasse, 91198 Gif-sur-Yvette, France; ²División Neurociencias, Laboratorio Andaluz de Biología, Universidad Pablo de Olavide, Ctra. de Utrera Km1, 41013, Sevilla, Spain; ³Institut de Génétique et de Biologie Moléculaire et Cellulaire, CNRS/INSERM/ULP, BP 10142 -67404 Illkirch Cedex, CU de Strasbourg, France

Abstract

Respiration is a rhythmic motor behavior that appears in the fetus and acquires a vital importance at birth. It is generated within central pattern-generating neuronal networks of the hindbrain. This region of the brain is of particular interest since it is the most understood part with respect to the cellular and molecular mechanisms that underlie its development. *Hox* paralogs and *Hox*-regulating genes *kreisler/mafB* and *Krox20* are required for the normal formation of rhombomeres in vertebrate embryos. From studies of rhombomeres r3 and r4, the authors review mechanisms whereby these developmental genes may govern the early embryonic development of para-facial neuronal networks and specify patterns of motor activities operating throughout life. A model whereby the regional identity of progenitor cells can be abnormally specified in r3 and r4 after a mutation of these genes is proposed. Novel neuronal circuits may develop from some of these misspecified progenitors while others are eliminated, eventually affecting respiration and survival after birth.

Index Entries: Hindbrain; rhombomeres; development; respiration; central pattern generators; transcription factor; *kreisler*; *Krox20*; *Hoxa-1*.

Received February 27, 2003; Accepted June 11, 2003

* Author to whom all correspondence and reprint requests should be addressed. E-mail: Christelle. Thaeron-Antono@iaf.cnrs-gif.fr

Introduction

How the respiratory rhythm is generated is a fascinating problem that has interested cellular neurobiologists, medical scientists, and comparative physiologists (1). The rhythmic respiratory-related neuronal network has been located within the hindbrain, in the pons, and the medulla. It is active before birth and controls respiratory-like rhythmic movements that are among the earliest detectable behaviors of the mammalian fetus. It becomes vital after birth and its impairment may contribute to sudden infant death syndrome that is the primary cause of death between 1 mo and 1 yr of age in developed countries (2). The analysis of human diseases with aberrant control of ventilation led to the hypothesis of a genetic control of breathing which, however, remains difficult to differentiate from confounding environmental factors. Genetic mechanisms postulated from studies of human twins (3), familial aggregation (4), and inbred mice strains (5) remain to be elucidated. The basis of variation of respiratory parameters in mammalian species is also unknown (6). This review specifically examines genes that affect respiratory parameters such as frequency, by controlling the organization of the central rhythmic neuronal network. Studies of the early stages of development in vertebrate evolution indicate that the respiratory circuit may be under the same genetic constraints and factors that are involved in early-hindbrain patterning.

In all vertebrates, the hindbrain is one of the vesicles that appears towards the anterior end of the neural tube. The hindbrain neuroepithelium becomes partitioned into an iterated series of cellular compartments along the antero-posterior axis, which are called rhombomeres (r1–r8). Segmentation is transient. It appears during the second half of the first month in humans, between E8 and E12 in mice, between stages 9 and 24 in chicks, and influences later differentiation and spatial distribution of neuronal patterns. For instance, the branchiomotor neurons of the cranial nerves conform to the

rhombomeric pattern with a two-segment periodicity (7). However, because segmentation is followed by the reconfiguration of neurons and synapses during fetal and postnatal stages, the impact of early rhombomeric patterns on the function of mature neuronal circuits remains to be established. Transcription factors that are expressed in rhombomere-specific patterns and are required for hindbrain segmentation and development have been identified. Among these are the homeobox genes of the *Hox* family and their regulators *Krox20* and *kreisler/mafB*.

Here, the authors first summarize available data on the molecular control of r3, r4, and adjacent rhombomeres and the involvement of the above transcription factors in hindbrain development. These data suggest that, according to the initial hypothesis of Lumsden (8), the spatially restricted patterns of developmental genes expression encode segment-specific positional information that is in turn translated into specific neuronal fates. Following an overview of the fetal and postnatal development of breathing, the authors present results indicating that the r3–r4 rhombomeric pair is required for the specification of neuronal circuits, breathing patterns, and survival.

Rhombomere-Specific Expression and Function of *Hox*, *kreisler/mafB*, and *Krox20* During Hindbrain Development

The *Hox* genes provide cells with positional information and identity along the antero-posterior axis of the embryonic body. Vertebrates display variable, species-specific numbers of *Hox* gene clusters originated by successive duplications of a single ancestral complex. Each cluster, in turn, contains variable numbers of tandemly organized transcriptional units, numbered from 1–13. *Hox* genes located in analogous position, but in different complexes, are named paralogs (i.e., *Hox* paralog group 1–13). They display similar, though not identical, expression patterns

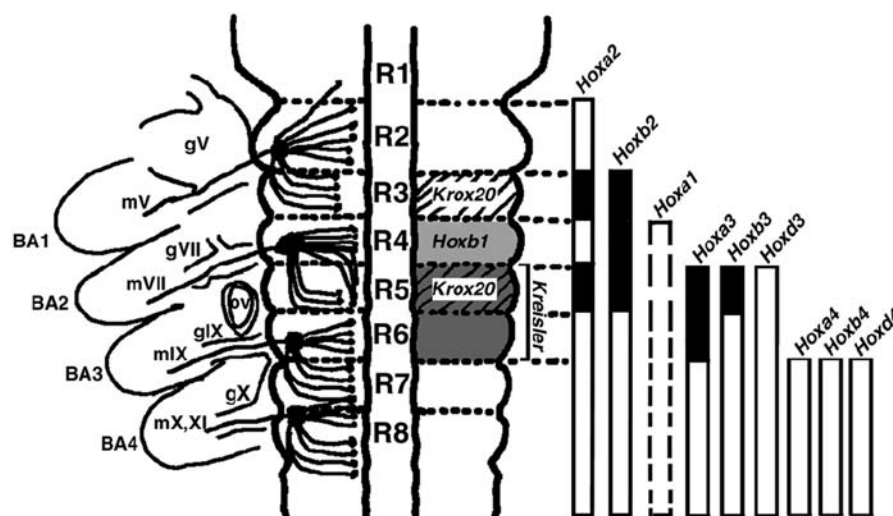


Fig. 1. Cranial nerve and gene expression patterns in the segmented hindbrain. The drawing shows a schematic flatmount representation of the mouse hindbrain and branchial arches at E10.5. The organization of cranial nerve motor nuclei and their projections is indicated on the left side. The segmental expression of *Krox20* (r3 and r5), *kreisler* (r5–r6), and *Hoxb1* (r4) is indicated on the right side. The rostrocaudal expression domains of *Hox* paralog groups 1–4 are shown as bars, adjacent to the hindbrain diagram. Each gene domain extends from the posterior end of the neural tube up to a sharp rostral boundary that maps precisely at rhombomere borders. However, *Hox* expression levels may not be homogenous along the rostrocaudal axis, displaying higher levels in some rhombomeres (black shading). Note that *Hoxa1* expression is only present at earlier stages up to the presumptive r3/r4 border, though not any longer at the segmentation stage (dashed bar). R, rhombomere; BA, branchial arch; ov, otic vesicle; mV–XI, motor component of cranial nerve V–XI; gV–X, sensory ganglia of cranial nerve V–X.

and partially redundant functions. In the hindbrain, *Hox* genes from paralog groups 1–4 show rhombomere-restricted expression (9,10; see Fig. 1). *Hox* expression is activated in the hindbrain neuroepithelium before segmentation, in response to inductive signals such as retinoic acid (11–13), and maintained through later developmental stages in neuronal progenitors and some postmitotic neurons (14–17). Analysis of loss- and gain-of-function mutations in mouse and chick embryos revealed an important role for *Hox* genes in the establishment of rhombomeric territories, the assignment of segmental identities, and rhombomere-specific neuronal patterns (9,10,16–31). Molecular and cellular analysis indicated also that neuronal differentiation is affected, or that the fate of certain neuronal progenitors is diverted to other subtype

identities. Morphological analysis has focused mainly on the branchiomotor neurons of the facial and trigeminal subtypes. In *Hoxa2* mutants, r2–r3 derived trigeminal branchiomotor neurons show abnormal axonal projections and branchial arch target selection (23). In contrast, in the absence of *Hoxb1* and *Hoxb2* functions, the development of the r4-derived facial nerve is impaired (16,17,20,21), and the fate of r4 facial branchiomotor progenitors is switched to serotonergic instead of cholinergic (32).

Interestingly, the initial establishment of the rhombomeric pattern does not follow a strict rostro-caudal order. Last year it was established that the presumptive r4 territory, in the center of the hindbrain neuroepithelium, is the first to be generated (33). In turn, the r4 territory acts as a local organizing center, signaling

to adjacent territories and starting a molecular cascade leading to the further partitioning into the r3, r5, and r6 segments (33,34). The expression of *Hox* paralog group 1 genes, *Hoxa1* and *Hoxb1*, is central to this process providing the earliest sign of r4 regionalization (10 and refs. therein). These genes are both expressed up to the presumptive r3/r4 boundary well before morphological segmentation. Subsequently, *Hoxa1* expression is downregulated whereas *Hoxb1* signal is maintained at high levels in r4 through an auto-regulatory loop. On the basis of analysis in zebrafish embryo, it could be suggested that the cooperative activity of *Hox* with their *Pbx* cofactors results in the upregulation of Fibroblast Growth Factor 3 (*Fgf3*) and *Fgf8* in r4, which in turn induce *kreisler/mafB* and *Krox20* in r5–r6 (33–36). *Hoxa1* function in r4 also contributes to the regulation of *Krox20* in r3, possibly via the activity of *Fgf* molecules from r4 (25,34). Indeed, this model is consistent with the analysis of single and compound *Hoxa1* and *Hoxb1* knockout mice (18–21,24,26). Specific hindbrain defects were observed, ranging from segmentation abnormalities to misspecifications of neurons. In particular, the *Hoxa1* single and *Hoxa1/Hoxb1* compound knockout mice resulted in abnormal rhombomere specification from r3 to r6. Altogether, these studies highlight the requirement of *Hox* genes and the dependence on inter-rhombomeric signaling for normal hindbrain segmentation and development.

The *kreisler* mutants were generated by X-ray mutagenesis. The homozygous mutant animals are hyperactive and their behavior is characterized by head-tossing, running in circles, and deafness due to absence of a functional inner ear (37–39). The *kreisler* mutation affects a *mafB*-related transcription factor, present in r5, r6, and in the roof plate along the hindbrain. *Kreisler/mafB* upregulates the expression of *Hoxa3* in both r5 and r6, and of *Hoxb3* in r5 (40,41). This is required for r5 formation since this rhombomere fails to form in *kreisler* homozygous mutants.

Within the yet unsegmented hindbrain, the *Krox20* gene is transiently expressed in two

stripes with sharp edges corresponding to the future rhombomeres r3 and r5 (42). *Krox20* acts as a direct transcriptional activator of other r3- and r5-related genes belonging to the homeobox clusters (43,44) and participates in rhombomere boundaries formation (45). The anatomical organization of the hindbrain and the expression patterns of rhombomere-specific genes demonstrate that the inactivation of *Krox20* in transgenic mice eventually eliminates r3 and r5 (46–48).

Respiratory Behavioral Patterns at Different Stages of Development

The vertebrate hindbrain displays variable, species-specific, reticular circuits producing rhythmic motor behaviors linked to the respiratory function in agnathian fishes (49), teleostean fishes (50), lungfishes (51), amphibians (52,53), reptiles (54), and birds (55). The rhythm can be episodic or permanent (56,57). In mammals, the postnatal respiratory rhythm characterizes permanent, bilaterally synchronized, and coordinated activities in spinal motor axons that innervate the diaphragm, inter-costal, and abdominal pump muscles as well as in cranial motor neurons that determine the flow resistance of the airways.

The generator responsible for the balanced sequence of inspiration, postinspiration (that slows lung deflation), and expiration (58,59) comprises a network of rhythmic “respiratory” reticular neurons, all located within the brainstem, which sequentially activate motoneurons during inspiration (e.g., phrenic motoneurons), postinspiration (e.g., expiratory recurrent laryngeal motoneurons), and expiration (e.g., internal intercostals motoneurons). The required neuronal patterns emerge from the interplay between synaptic relationships and electrical membrane properties that are identifiable by electrophysiological recording on rhythmically active preparations isolated in vitro (60–63). The regulatory loops for breathing involve sensory inputs from, for example, peripheral lung

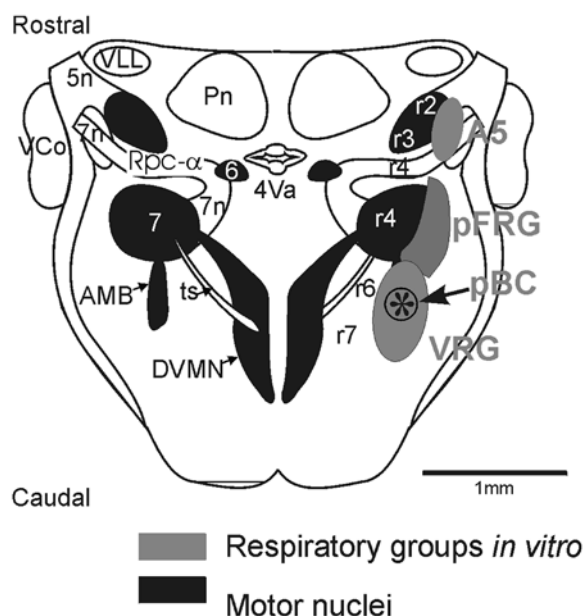


Fig. 2. Schematic representation of brainstem nuclei, ventral respiratory groups, and rhombomeres origin of branchiomotor nuclei and nerves. Schematic drawing of an horizontal section of the neonatal mouse brainstem. (A) Localization and name of the brainstem nuclei. 4Va: anterior part of the 4th ventricle; 5: trigeminal motor nucleus; 5n: trigeminal nerve; 6: abducens motor nucleus; 7: facial motor nucleus; 7n: facial nerve; AMB: ambiguus nucleus; DVMN: dorsal motor nucleus of the vagus; Pn: pons nucleus; Rpc- α : parvocellular reticular formation; ts: tractus solitarius; VCo: vestibular-cochlear nuclei; VLL: ventro-lateral lemniscus. (B) Localization of the ventral respiratory groups active in vitro. A5: pontine catecholaminergic group A5 (inhibitor of respiratory rhythm); pBC (star): preBötzinger complex; pFRG: para-facial respiratory group (67); VRG: ventral respiratory group. Rhombomeric origins of branchio-motor nuclei in mice are indicated: trigeminal motor nucleus is derived from r2/r3; facial motor nucleus and nerve are derived from r4, glossopharyngeal nucleus originates in r6/r7.

mechanoreceptors, carotid body chemoreceptors, and intracranial chemosensors.

An antero-posterior (AP) organization of the respiratory network was already recognized physiologically in 1923 (1) with the identifica-

tion of the most rostral Pontine Respiratory Group (PRG) in mammals, in vivo. Available data are interesting to confront with adult anatomical features that are specified by the AP pattern of *Hox* gene expression. For example, branchiomotor nuclei conform to the rhombomeric pattern (7,8). Trigeminal motoneurons originate from r2 and r3 and send their axons (5n in Fig. 2) to an exit point in r2. In mammals, the facial branchial nucleus originates in r4. The ventral (ambiguus, AMB in Fig. 2) and dorsal (DVMN in Fig. 2) motor nuclei of glossopharyngeal-vagal nerves derive from r6–r8. AP anatomical features are less obvious in the reticular formation. Nevertheless, the electrophysiological analysis of rhythm generation in vitro has been performed on rodent neonates and revealed respiratory-related systems in register with the general organization of branchiomotor nuclei. Caudally, at the vagal level, the neonatal inspiratory rhythm is generated in a subdivision of the ventral respiratory group (VRG in Fig. 2), the pre-Bötzinger complex (56; pBC in Fig. 2), and persists in coronal brainstem slices of newborn rodents, isolated in vitro (64,65). At the trigeminal level, ventral pontine controls of the rhythm (66) includes noradrenergic neurons of the A5 group exerting a depressant effect upon the caudal VRG (62). At the facial level, a distinct neonatal rhythm generator has recently been delineated by activity-dependent imaging and called the para-facial respiratory group (67; pFRG in Fig. 2). In contrast to the inspiratory pBC, the pFRG is characterized by a pre-inspiratory pattern of neuronal activity stopping during inspiration and resumed afterward by a postinhibitory rebound. It seems that potent respiratory depressants such as opioids (68–70) act in neonates by disrupting the balanced pFRG-pBC interaction that is required for permanent rhythm generation in the hindbrain isolated in vitro (67,71). The respiratory network is also organized along the dorso-ventral axis. The pFRG, the pBC, and the A5 group (Fig. 2) lie ventrally. There is no respiratory-related neuronal groups lying dorsally in the trigeminal and facial domains of the hindbrain (see Generation of a Novel Functional Circuit in

the Dorsal Pons of *Hoxa1* Mutant Mice 4). The dorsal part of the network contains rostrally, the PRG (at a r1-derived position) and caudally, part of the nucleus tractus solitarius where r6–r8-derived sensory afferents of the tractus solitarius (ts in Fig. 2) terminate. This dorsal part of the network plays a role in vivo in the transition from inspiration to postinspiration, but it does not function normally in vitro (72). Thus, this review concentrates on ventral respiratory groups, particularly those located within the r3/r4-derived domains.

Fetal Breathing

In the late fetal period, such an organization of the respiratory networks forming discrete cell groups is also found. Analysis of fetal lamb in vivo has revealed powerful rostral pontine inhibitory mechanisms that are brought into play by maturation of sleep states and causes periodic breathing until birth (73). Differences between fetal and adult breathing behavior in mammals reveal the extent of maturational changes that continue after birth (74,75). Fetal breathing is part of a global stereotyped movement pattern including startle, hiccuping, limb movements, and head retroflexion. In humans, this pattern starts at the beginning of the third month of pregnancy and increases in complexity and frequency afterward (76). In mice, coordinated rhythmic movements of the rib cage, opening of the mouth, and flexion of the neck and body start at E15.5 (77). However, before E18 in rats, typical features of the rhythmic hindbrain in vitro are lacking, particularly the predominance of hindbrain over spinal rhythms, the effect of the A5 group, and the central sensitivity of the hindbrain to CO₂ (62,78). Therefore, although there are major maturational steps at mid-fetal stages, rhythm generation itself starts much earlier.

Primordial Rhythm Generation

Electrophysiological recordings performed on an isolated preparation of chick embryo hindbrain revealed that by the end of the seg-

mentation period (stage 24), the hindbrain neuronal network starts to exhibit a consistent and organized activity in the form of recurring episodes composed of burst discharges that occur simultaneously in the different cranial nerves (79). At this stage the neuronal network is already organized with distinct reticular and motor neurons. Cross-correlation analysis of primordial activities recorded in the trigeminal, facial, and glossopharyngeal rootlets demonstrate that the different motoneuronal pools along the AP axis are coactivated through multisynaptic reticular relationships (80). When intersegmental relationships are interrupted by transverse sectioning of the hindbrain rostral and caudal to the exit of the branchiomotor nerve, the ability to generate the rhythmic pattern is preserved in each transverse slice. Thus, each pair of rhombomeres, particularly the para-facial segment originating from r4–r5, contains its own rhythm generator (80).

Hoxa1, kreisler/mafb, and Krox20 Control Rhombomere-Specific Regional Identity of Neural Precursors

Neurons in different rhombomeres probably differ in membrane electrical properties or network organization, in agreement with the proposed role of segmentation in the supply for neurobiological substrates with both redundant elements and discrete variations in local properties. At stage 18 in chick, a set of 8 reticular neuronal phenotypes has been characterized in chick rhombomeres from their pattern of axonal trajectories (81), providing an anatomical basis for the coactivating system. Clonal analysis after intracellular labeling of single cells at stages 7–8 revealed that determination of ultimate neuronal phenotypes may occur already in precursor cells, before the end of mitotic divisions (82). Such early phenotypic choices would also be determinant in conferring electrophysiological properties, such as the ability to generate a rhythm.

Within the yet unsegmented hindbrain, cells can be characterized by selective expression patterns of rhombomere-specific molecular markers. Evidence for early phenotypic choices during development came recently from the analysis of mutation-induced discrepancies between the actual location of precursor cells and their genetically-specified regional identity. For example, in *Hoxa1*^{-/-} mutants, ectopic patches of cells displaying an r2-like identity were found at the r4 axial level (83). This is remarkably similar to what is also observed in *Hoxb1*^{-/-} mice (20) and in the compound *Hoxa1/Hoxb1* double mutant (84), congruent with the notion that *Hoxb1* is a downstream target of *Hoxa1* (12,85,86). In addition, patches of r2-like cells were also present at the level of r3 in *Hoxa1*^{-/-} mutants (25,83). Thus, in the absence of *Hoxa1*, some neural precursors at the presumptive r3–r4 level acquire an r2 identity, whereas others maintain their appropriate molecular programs. This partial anteriorization of the cellular phenotype could be induced by lack of *Hoxb1* activation in pre-r4 cells.

Misspecification of cell positional identity has been also observed after the inactivation of *Hox*-regulating factors. For example, in heterozygous (+/*kr*) and homozygous (*kr/kr*) *kreisler* mutant embryos, posteriorization of the cellular phenotype is observed in r3. This is probably due to the ectopic expression of *kreisler/mafB* itself and of its target *Hoxa3* in r3, both normally expressed posterior to the r4/r5 boundary (41,87,88). Moreover, in *Krox20*-null mutant embryos, analysis of even-numbered rhombomere molecular markers demonstrated that r3 cells acquire r2 or r4 identity, and r5 cells acquire r6 identity (89). Initial activation of *Krox20* in a few cells leads to the segregation, homogenization, and possible expansion of territories to which *Krox20* confers an odd-numbered identity (45).

Interestingly, populations of misspecified progenitor cells are not necessarily eliminated during later developmental stages. To investigate the developmental fate of ectopic r2-like precursors in *Hoxa1*^{-/-} mutants, cell-migration

patterns were examined (83). In wild-type E11.5 embryos, facial motoneurons born in r4 migrate caudally through r5 into r6 to form the facial motor nucleus, whereas trigeminal motoneurons migrate dorso-laterally in r2 and r3. In the *Hoxa1*^{-/-} mutant r4 region, a reduced number of facial motoneurons migrate caudally and an abnormal trigeminal-like dorso-lateral migration of r4 cells is detected at E11.5 and completed at about E12.5. Remarkably, lack of caudal migration of facial motoneurons and lateral trigeminal-like migration are also observed in *Hoxb1*^{-/-} mice (20). Thus, neurons with an anteriorized trigeminal-like phenotype appear to survive at the facial level of *Hoxa1* mutant hindbrains. These observations give insights into some of the mechanisms underlying early phenotypic choices that affect neuronal progeny at later developmental stages. They also provide animal models to evaluate after birth the physiological significance of these phenotypic choices in rhythm-generating neuronal networks of the hindbrain reticular formation.

Generation of a Novel Functional Circuit in the Dorsal Pons of *Hoxa1* Mutant Mice

Analysis of the breathing pattern using plethysmographic methods *in vivo*, revealed an abnormal behavioral control in *Hoxa1*^{-/-} and +/*kr* mutant neonates that might result from abnormal specification of r3 and r4 cells during early development (83,90). Rhombomere (r4) elimination in *Hoxa1*^{-/-} mutants correlates with a low neonatal respiratory frequency and death within 2.5 h (see Vital Role of a Para-Facial Anti-Apneic Neuronal System). However, *Hoxa1*^{-/-} newborns exhibiting a higher frequency at birth and major respecifications in r3 and r4, progressively increased their respiratory rate to normal values and survived for about 18 h (see Fig. 6B/C in ref. 83). Furthermore, comparison between wild-type and +/*kr* mutant mice provided the first description of

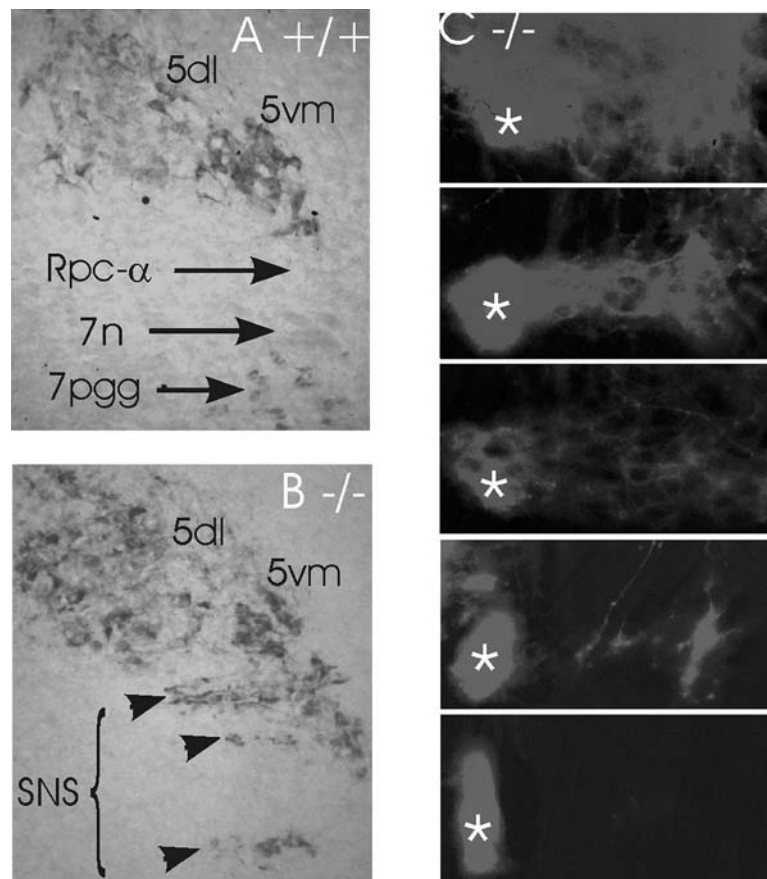


Fig. 3. Anatomical location of the dorsal pontine *Hoxa1*^{-/-} supernumerary neuronal structure (SNS) at birth. Rhombomeres are polyclonal developmental units in which a large variety of neuronal types develop. Therefore the *Hoxa1*^{-/-} mutation not only affects reticular neurones: motoneurons provide important landmarks for the localization of anatomical deficits. (A,B) Horizontal sections of the dorsal pons showing cholineacetyltransferase immunoreactive pontine neurons in WT (A) and *Hoxa1*^{-/-} (B) in the dorso lateral (5dl) and ventro medial (5vm) trigeminal motor nucleus and adjacent areas. Supernumerary motor nuclei nos. 1, 2, and 3 (from top [anterior] to bottom [posterior]) arrowheads in (B) are localized in the extended Rpc-α, at the level of the eliminated intracranial facial nerve (7n) and preganglionic facial neurons (7pgg). (C) Adjacent horizontal sections from dorsal (top) to ventral (bottom), showing retrograde Dil labelling the SNS motor nucleus no. 2 in an *Hoxa1*^{-/-} mutant mouse. More ventral views (bottom) show a supernumerary dorso-ventral fasciculus (star) located laterally in subnucleus no. 2 and distinct from the WT-like trigeminal root located more rostrally (not shown).

an increased respiratory frequency congruent with abnormal cell specifications in r3 that are not associated with rhombomere elimination and lethality (90). Thus, one possibility is that misspecification of neuronal fates in mutant r3 and r4 might lead to rhythm controlling neuronal circuits that enhance survival rates by significantly increasing frequency values.

Identification of these circuits in *Hoxa1*^{-/-} mutants required a combination of anatomical and in vitro physiological approaches.

In keeping with the abnormalities of the r3–r4 region at early developmental stages, the *Hoxa1*^{-/-} mutation reorganized the anatomy of the Parvocellular Reticular Formation pars alpha (Rpc-α in Figs. 2 and 3A), which was

extended along the A-P axis. In addition, radial stripes of reticular formation and ectopic motoneurons alternate, forming a compound reticular and motor supernumerary neuronal structure (SNS in Fig. 3A). Ectopic motoneurons formed 3 distinct subnuclei (arrowheads in Fig. 3B) and a distinct dorso-ventral motor fasciculus running laterally, caudal to the normal trigeminal root (Fig. 3C). Therefore, abnormal cell specification in r3 and r4 leads, in the *Hoxa1*^{-/-} dorsal pontine domain, to the formation of 3 motor subnuclei alternating with stripes of reticular formation at the same location as the wild-type *Rpc-α*.

To identify the function of these reticular neurons, the hindbrain was isolated in vitro during the first postnatal days (P0–P1) and the dorsal pons was exposed in a thick horizontal slice, and made accessible to dorsal approach under microscopic control (83). This slice preparation also included the bilateral pBC (stars in Fig. 4) that generates a persisting rhythmic activity propagating to cranial (e.g., trigeminal) motor neurons from which it can be recorded. The SNS was stimulated by pressure application of the glutamatergic agonist α -amino-3-hydroxy-5-methyl-4-isoxazolepropionic acid (AMPA). The contralateral trigeminal nerve (5n in Fig. 4) was recorded to avoid direct stimulation of motoneurons.

The *Rpc-α* is a dorsal pontine structure normally lacking respiratory-related functions (91; see Respiratory Behavioral Patterns at Different Stages of Development). Therefore, AMPA applications had no effect on rhythm frequency in the wild-type preparations. By contrast, in the mutant SNS, AMPA induced a robust increase in rhythm frequency, followed in all cases by a transient inhibition of the rhythm (Fig. 4). In the mutants, labeling the VRG with Dil revealed a robust axonal pathway, not present in the wild-type, and running laterally in the mutant pons (83). These results strongly suggest the presence of supernumerary functional efferent connections of the SNS to the rhythm generator (83). Moreover, rhythmic activity recorded from single neurons in the SNS area also indicated afferent connec-

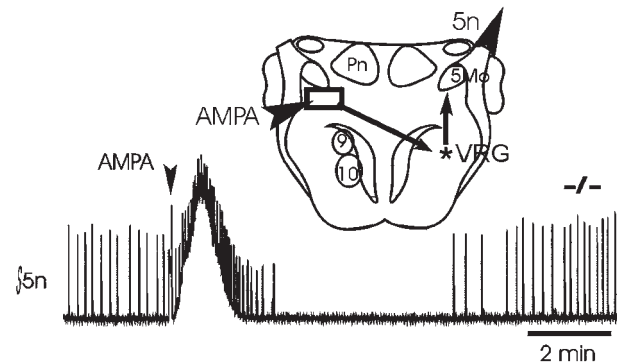


Fig. 4. Functional connectivity of reticular neurons in the *Hoxa1*^{-/-} supernumerary neuronal structure (SNS) at birth. (A) Schematic presentation of the slice preparation. Arrows: supernumerary connections in mutants from SNS (rectangle) to the rhythm generator (star); rectangle shows the approximate extent of the area affected by AMPA (α -amino-3-hydroxy-5-methyl-4-isoxazolepropionic acid) applications (arrowhead, more medial applications were ineffective). (B) Modification of the contralateral trigeminal nerve activity (5n) induced by exciting SNS neuronal cell bodies using brief (25 ms) pressure applications of AMPA in *Hoxa1*^{-/-} hindbrain slices in vitro. Burst (upward deflections) frequency is significantly increased and decreased indicating a functional connection to the rhythm generator in *Hoxa1*^{-/-}. This response is not seen in WT mice (83). 5n: trigeminal nerve; 5Mo: trigeminal motor nucleus; 9: glossopharyngeal nucleus; 10: vagus nucleus; Pn: Pontine nucleus; VRG: ventral respiratory group.

tions from the rhythm generator. Thus, in *Hoxa1*^{-/-} mutant mice, the SNS exhibits a novel relationship with the respiratory rhythm generator, while preserving premotor *Rpc-α* connections with the trigeminal system.

Altogether, the anatomo-functional analysis indicates that the *Hoxa1* mutation reorganizes the dorsal pons where a neuronal circuit, originating from the mutant r3–r4 region, is incorporated into the hindbrain neuronal network. As a consequence, the animal acquires a novel in vitro respiratory-promoting function, enhancing survival for several hours, although unable to abolish lethality of the *Hoxa1*^{-/-} phenotype.

Vital Role of a Para-Facial Anti-Apneic Neuronal System

As shown above, phenotypic choices in r3 and r4 seem to initiate development of reticular circuits that stimulate respiratory rhythm generation. Respiratory consequences of the elimination of r3 and r4 in different mutants confirmed that these circuits are of vital physiological significance in mice during the first days after birth. Life-threatening deficiency of a central rhythm promoting system has been first described after the elimination of r3 and r5 in *Krox20*^{-/-} mice (92). This system, named “the anti-apneic system,” has been located in the caudal pontine reticular formation by recording rhythmic activity from the isolated hindbrain.

Integrity of r3 and r4 Is Required for Survival After Birth

In vivo, *Krox20*^{-/-} neonates with impaired anti-apneic function show an abnormally low respiratory frequency and apneas lasting 10× longer than normal. Most of the animals die during the first 2 d after birth. The *Krox20*^{-/-} mutants do not allow to distinguish between r3 and r5. Nevertheless, observations of *kr/kr* mice indicate that the fate of neurons greatly differs in r3 and r5. In contrast to *Hoxa1*^{-/-} and *Krox20*^{-/-} mutants, *kr/kr* mice exhibit no life-threatening apneic pattern of breathing despite elimination of r5 and dramatic hypoplasia of the pontine reticular formation leading to an abnormal positioning of the ambiguus nucleus (90). Therefore, the anti-apneic system specified in r3 and r4 retain a vital importance for breathing after birth, while neurons specified in r5 do not.

All *Hoxa1*^{-/-} mutants die from central respiratory deficits and terminal apnea and the morphological analysis indicates a rather extensive cellular reorganization affecting ventrally the size of the reticular formation (83). A 40% reduction of the length of the ventral pons results from the hypoplasia of r4- and r5-derived structures (SO, 7Mo in Fig. 5), including the pFRG which, therefore, seems to be

essential for a stable, high frequency rhythm generation. Thus, comparison with *kr/kr* mutants suggests that apneas and lethality in *Hoxa1*^{-/-} and *Krox20*^{-/-} mutants result from the elimination of para-facial reticular structures originating from r4 and r3 respectively.

Naloxone Administration Improves Survival of *Krox20*^{-/-} and *Hoxa1*^{-/-} Mutants

In an attempt to improve survival of *Krox20*^{-/-} mutants, CO₂ and naloxone were used to respectively increase chemosensory stimulation or decrease opioid inhibition of the respiratory rhythm during the first postnatal day. The partial pressure of CO₂ in the arterial circulation, sensed by peripheral and central chemoreceptors, is a major chemical drive of respiration. Thus, *Krox20*^{-/-} animals were exposed to a CO₂-enriched (4%) atmosphere during the severe apneic syndrome. The respiratory frequency was increased only for the duration of the CO₂ exposure and no stable improvement of the breathing pattern was obtained (92). Naloxone is an antagonist for μ and δ receptors through which opioid peptides exert a depressant modulatory control of respiratory rhythm (58) and impair interactions between pFRG and pBC respiratory oscillators (71). Subcutaneous naloxone administration to *Krox20*^{-/-} and *Hoxa1*^{-/-} animals increased the respiratory frequency for several hours. Furthermore, naloxone treatment definitively suppressed the occurrence of apneas and eliminated lethality during the first postnatal week (83,92). An apneic-like rhythmic activity is characterized in vitro by long periods during which the *Hoxa1*^{-/-} slice preparation is inactive. Naloxone administration suppresses selectively these silent periods (see Fig. 6). Observations in vivo and in vitro therefore indicate that neuromodulation by endogenous opioids contributes to the generation of life-threatening apneas that develop after impairment of the anti-apneic system, and that antagonists of the opioid neuro-transmission might provide effective pharmacological tools to be used when the neonatal anti-apneic function is disrupted.

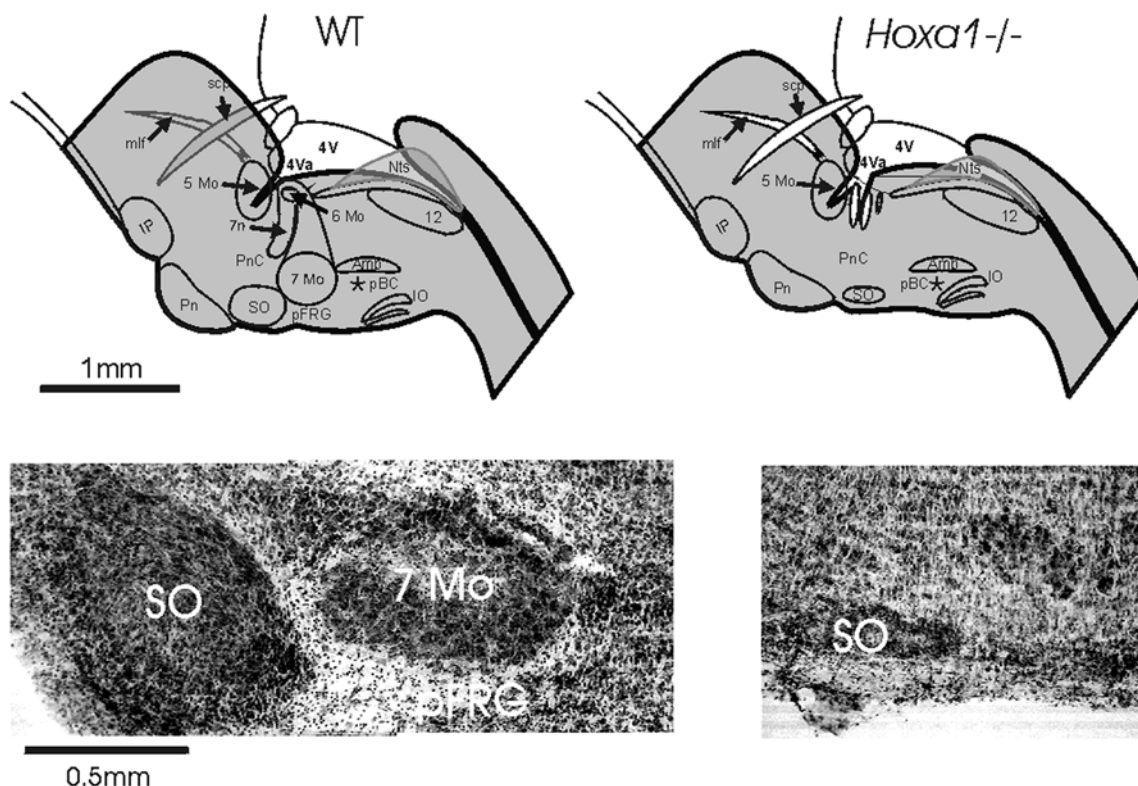


Fig. 5. Ventral pontine hypoplasia in *Hoxa1*^{-/-} mutants shown in sagittal sections of the hindbrain. Parasagittal sections of the hindbrain at PO in WT (left) and *Hoxa1*^{-/-} (right) littermates. (A) Drawings of the entire hindbrain. (B) Lateral sections showing the ventral half of the pons extending from the rostral pole of the superior olivary (SO) to the caudal pole of the facial motor nucleus (7Mo). Note the dramatic hypoplasia of the ventral pons along the antero-posterior axis, affecting the area of the pFRG. Drawings, including the analysis of 5 *Hoxa1*^{-/-} mice, include both lateral and medial structures; medial sections (in gray) show dorsal group of anomalies affecting the ventricular surface and the supernumerary neuronal structure. 4V: fourth ventricle; 4Va: anterior part of the fourth ventricle; 5Mo: trigeminal motor nucleus; 6Mo: abducens motor nucleus; 7Mo: facial motor nucleus; 12: hypoglossal nucleus; Amb: ambiguus nucleus; IO: inferior olive; IP: interpeduncular nucleus; mlf: medial longitudinal fasciculus; Nts: nucleus tractus solitarius; pBC (star): preBötzinger complex; pFRG: para-facial respiratory group; Pn: pontine nucleus; PnC: caudal pontine nucleus; scp: superior cerebellar peduncle (brachium conjunctivum).

Rhythm Controlling Systems Deriving From the r3–r4 Hindbrain Level

Assembling a Rhythm-Promoting Neuronal Network in Chick r3 and r4

As described above, a modification of the *Hox* expression pattern in r3 and r4 is sufficient to incorporate a novel neural control in the

mature hindbrain, suggesting that regulatory changes in adjacent rhombomeres r3 and r4 may be required for the generation of para-facial circuits controlling the respiration rhythm. Interestingly, assembling of a rhythm-promoting respiratory network also requires the two-segment functional unit r3–r4 in the chick (93). From the close of the segmental period in the chick embryo, (stage 24) until stage 28 (E4.5–5.5), the isolated hindbrain gen-

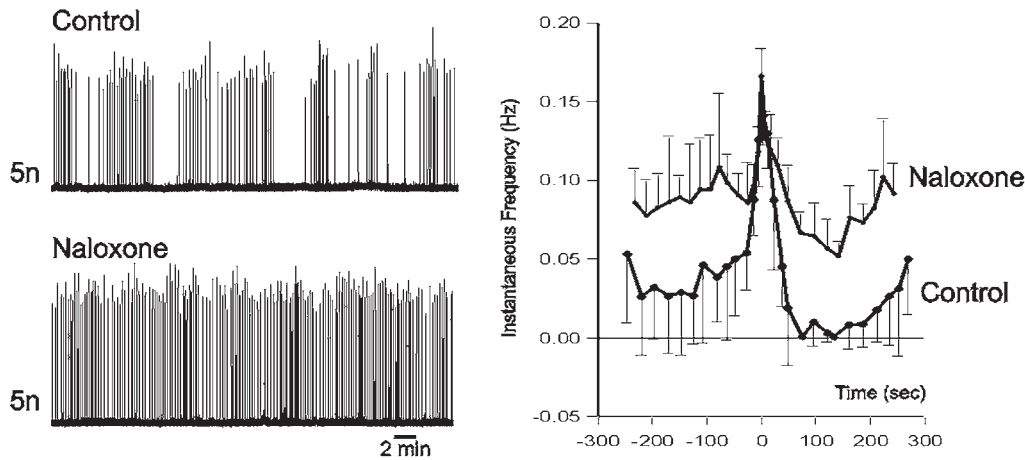


Fig. 6. Naloxone alleviates the apneic-like pattern of rhythmic activity generated by an *Hoxa1*^{-/-} hindbrain isolated in vitro. Same experimental procedure as in Fig. 4; abnormal rhythmic pattern characterized by long inter-burst intervals alternating with periods of higher frequency during perfusion of the slice with a naloxone-free medium. Average changes in frequency (in ordinates) around peak-burst frequencies (taken as time zero in the abscissa) are shown on the right. This pattern resembles the periodic respiratory pattern described in the lamb fetus *in utero* (84). Bath application of naloxone (1 μ M, 5 min) eliminates long interburst intervals. This mechanism is probably responsible for the naloxone-induced elimination of apneas in vivo. 5n: trigeminal nerve.

erates a low frequency primordial rhythmic pattern, with inter-burst intervals of more than 1 min. This is also seen in mice at E12. These frequencies are one order of magnitude lower than fetal and neonatal rhythms. A more mature activity with high frequency episodes appears at around E6 in chick and E13.5 in mouse (94). Electrophysiological analysis in chick revealed that onset of this episodic pattern coincides with the appearance of rhythmic inhibitions (93) resembling those recorded in pFRG neurons (63,67). The early establishment of this episodic central pattern prompted investigation of its origin in relation to hindbrain segmentation. This was done by recording activities at E7–7.5, from brain territories deriving from individual or pairs of rhombomeres isolated *in situ* at the time of their formation (E2). The r3r4 pair developed a normal episodic rhythm, while isolated r2, r4, and r2r3, r4r5 pairs did not. Therefore, r3 appears to be required for the generation of an episodic neuronal pattern in the caudal para-facial neighbor r4 or r4r5 (93). Altogether, experi-

ments in mouse and chick show that perturbations of the rhombomeric patterning in r3 and r4 irreversibly alter the function of the para-facial neuronal network and can be reflected at birth by respiratory deficits.

Relevance for Life-Threatening Congenital Syndromes Affecting Respiration in Infants

Experiments on the sheep fetus *in utero* (95,96) demonstrate regular continuous breathing during early fetal development. In later stages fetus exhibits sleep apneas typical of the irregular respiratory pattern at birth. Because pontine surgical lesions restore continuous breathing, apneas were attributed to the development of a rostral control. Thus, para-facial anti-apneic neurons affected by the *Krox20* and *Hoxa1* mutations may counteract this control by turning the respiratory rhythm from intermittent to more continuous breathing in an opioid-sensitive manner. Such a role appears to be of vital importance at birth during a pre-

cise time window, extending in mice during the first 2 d after birth.

Therefore, the *Hoxa1* and *Krox20* mutant mice are of potential interest as animal models for pathophysiological studies. In humans, life-threatening apneas during early infancy result from a number of to date poorly understood etiologies including dysfunction of brainstem mechanisms (97,98) and patterns of segmental, homeobox-like, brainstem lesions (99). Distinct reflex reactions generated at different levels of the brainstem and observed in mice models point out at least 3 distinct syndromes indicative of abnormal embryonic development of hindbrain circuits. They might be detectable in human by scoring simple reflex reactions such as chemosensory reflexes affected in human congenital central hypoventilation syndrome (100,101) or the righting reflexes affected by *kr/kr* or *Hoxa1*^{-/-} syndromes (102). A failure of airways protective and startle reflexes during sleep of human infants in a prone position, is also suspected in the sudden death syndrome (103). Defects of the startle reflex may be part of the *kr/kr* or *Hoxa1*^{-/-} syndromes or result from the elimination of r3-derived giant pontine reticular neurons eliminated by the *Krox20*^{-/-} mutation (92). Suction involves trigeminal premotor interneurons located in the Rpc- α (91). These dorsal pontine neurons are likely derived from r3, since Rpc- α is eliminated in *Krox20*^{-/-} mutants, which in addition exhibit an abnormal suction behavior after birth (92). In contrast, abnormalities of r4 in *Hoxa1*^{-/-} animals do not affect suction, indicating that developmental processes in r3 and r4 differentially affect the feeding behavior. These findings have considerable significance both on developmental and evolutionary grounds, indicating that hindbrain segmentation, particularly at the r3/r4 level, is essential for the normal development of adaptive behaviors controlled by the brainstem. The evolution of neural networks of multisegmental origin may be facilitated by the partitioning of the early hindbrain in a number of rhombomeric units initially developing as independent modules (8,81,104). Furthermore, because transcription factors orchestrating

hindbrain segmentation are organized in a regulatory network, a single mutation may have several consequences, so that prediction of neuronal deficits in patients is not straightforward. A point mutation may not necessarily eliminate function of neurons. Genetic abnormalities of hindbrain segmentation are potentially able to suppress (*kr/kr*, *Krox20*^{-/-}) or enhance (*+/kr*, *Hoxa1*^{-/-}) the function of respiration controlling neuronal system.

Acknowledgment

Work in Jean Champagnat's and Filippo M. Rijli's laboratories are supported by grant QLG2-CT-2001-01467 "Brainstem Genetics." Eduardo Dominguez del Toro was supported by CEE (BIO4-CT975-096) and FRM (EP001227/1) training grants.

References

1. Lumsden T. L. (1923) Observation on the respiratory centres in the cat. *J. Physiol.* **57**, 153–160.
2. Harper R. M., Kinney H. C., Fleming P. J., and Thach B. T. (2000) Sleep influences on homeostatic functions: implications for sudden infant death syndrome. *Respir. Physiol.* **119**(2–3), 123–132.
3. Kobayashi S., Nishimura M., Yamamoto M., Akiyama Y., Kishi F., and Kawakami Y. (1993) Dyspnea sensation and chemical control of breathing in adult twins. *Am. Rev. Respir. Dis.* **139**, 1192–1198.
4. Redline S. R. and Tishler P. V. (2000) The genetics of sleep apnea. *Sleep Med. Rev.* **4**, 583–602.
5. Tankersley C. G., Fitzgerald R. S., Levitt R. C., Mitzner W. A., Ewart S. L., and Kleeberger S. R. (1997) Genetic control of differential baseline breathing pattern. *J. Appl. Physiol.* **82**, 874–881.
6. Mortola J. P. (1987) Dynamics of breathing in newborn mammals. *Physiol. Rev.* **67**, 187–234.
7. Lumsden A. and Keynes R. (1989) Segmental patterns of neuronal development in the chick hindbrain. *Nature* **337**, 424–428.
8. Lumsden A. (1990) The cellular basis of segmentation in the developing hindbrain. *TINS* **13**, 329–335.

9. Lumsden A. and Krumlauf R. (1996) Patterning the vertebrate neuraxis. *Science* **274**, 1109–1115.
10. Rijli F. M., Gavalas A., and Chambon P. (1998) Segmentation and specification in the branchial region of the head: the role of the *Hox* selector genes. *Int. J. Dev. Biol.* **42**, 393–401.
11. Dupe V., Davenne M., Brocard J., Dolle P., Mark M., Dierich A., Chambon P., and Rijli F. M. (1997) In vivo functional analysis of the *Hoxa-1* 3' retinoic acid response element (3'RARE). *Development* **124**(2), 399–410.
12. Studer M., Gavalas A., Marshall H., Ariza-McNaughton L., Rijli F. M., Chambon P., and Krumlauf R. (1998) Genetic interactions between *Hoxa1* and *Hoxb1* reveal new roles in regulation of early hindbrain patterning. *Development* **125**, 1025–1036.
13. Gavalas A. and Krumlauf R. (2000) Retinoid signalling and hindbrain patterning. *Curr. Opin. Genet. Dev.* **10**(4), 380–386.
14. Graham A., Maden M., and Krumlauf R. (1991) The murine *Hox-2* genes display dynamic dorsoventral patterns of expression during central nervous system development. *Development* **112**(1), 255–264.
15. Tiret L., Le Mouellic H., Maury M., and Brulet P. (1998) Increased apoptosis of motoneurons and altered somatotopic maps in the brachial spinal cord of *Hoxc-8* deficient mice. *Development* **125**, 279–291.
16. Davenne M., Maconochie M. K., Neun R., Pattyn A., Chambon P., Krumlauf R., and Rijli F. M. (1999) *Hoxa2* and *Hoxb2* control dorsoventral patterns of neuronal development in the rostral hindbrain. *Neuron* **22**, 677–691.
17. Gaufo G. O., Flodby P., and Capecchi M. R. (2000) *Hoxb1* controls effectors of sonic hedgehog and *Mash1* signaling pathways. *Development* **127**, 5343–5354.
18. Mark M., Lufkin T., Vonesh J. L., et al. (1993) Two rhombomeres are altered in *Hoxa-1* mutant mice. *Development* **119**, 319–338.
19. Carpenter E. M., Goddard J. M., Chisaka O., Manley N. R., and Capecchi M. R. (1993) Loss of *Hoxa1* (*Hox-1.6*) function results in the reorganization of the murine hindbrain. *Development* **118**, 1063–1075.
20. Studer M., Lumsden A., Ariza-McNaughton L., Bradley A., and Krumlauf R. (1996) Altered segmental identity and abnormal migration of motor neurons in mice lacking *Hoxb-1*. *Nature* **384**, 630–634.
21. Goddard J. M., Rossel M., Manley N. R., and Capecchi M. R. (1996) Mice with targeted disruption of *Hoxb-1* fail to form the motor nucleus of the VIIth nerve. *Development* **122**, 3217–3228.
22. Barrow J. R. and Capecchi M. R. (1996) Targeted disruption of the *Hoxb-2* locus in mice interferes with expression of *Hoxb-1* and *Hoxb-4*. *Development* **122**(12), 3817–3828.
23. Gavalas A., Davenne M., Lumsden A., Chambon P., and Rijli F. M. (1997) Role of *Hoxa-2* in axon pathfinding and rostral hindbrain patterning. *Development* **124**, 3683–3691.
24. Gavalas A., Studer M., Lumsden A., Rijli F. M., Krumlauf R., and Chambon P. (1998) *Hoxa1* and *Hoxb1* synergize in patterning the hindbrain, cranial nerves and second pharyngeal arch. *Development* **125**, 1123–1136.
25. Helmbacher F., Pujades C., Desmarquet C., Frain M., Rijli F. M., Chambon P., and Charnay P. (1998) *Hoxa1* and *Krox-20* synergize to control the development of rhombomere 3. *Development* **125**, 4739–4748.
26. Rossel M. and Capecchi M. R. (1999) Mice mutant for both *Hoxa1* and *Hoxb1* show extensive remodeling of the hindbrain and defects in craniofacial development. *Development* **126**, 5027–5040.
27. Jungbluth S., Bell E., and Lumsden A. (1999) Specification of distinct motor neuron identities by the singular activities of individual *Hox* genes. *Development* **126**, 2751–2758.
28. Bell E., Wingate R. J., and Lumsden A. (1999) Homeotic transformation of rhombomere identity after localized *Hoxb1* misexpression. *Science* **284**, 2168–2171.
29. Barrow J. R., Stadler H. S., and Capecchi M. R. (2000) Roles of *Hoxa1* and *Hoxa2* in patterning the early hindbrain of the mouse. *Development* **127**(5), 933–944.
30. Pasqualetti M., Neun R., Davenne M., and Rijli F. M. (2001) Retinoic acid rescues inner ear defects in *Hoxa1* deficient mice. *Nat Genet.* **29**(1), 34–39.
31. Pasqualetti M. and Rijli F. M. (2001) Homeobox gene mutations and brain-stem developmental disorders: learning from knockout mice. *Curr Opin Neurol.* **14**(2), 177–184.
32. Pattyn A., Vallstedt A., Dias J. M., Samad O. A., Krumlauf R., Rijli F. M., Brunet J. F., and Ericson J. (2003) Coordinated temporal and spatial control of motor neuron and serotonergic neuron generation from a common pool of CNS progenitors. *Genes Dev.* **17**(6), 729–737.

33. Maves L., Jackman W., and Kimmel C. B. (2002) FGF3 and FGF8 mediate a rhombomere 4 signaling activity in the zebrafish hindbrain. *Development* **129**, 3825–3837.
34. Walshe J., Maroon H., McGonnell IM., Dickson C., and Mason I. (2002) Establishment of hindbrain segmental identity requires signaling by FGF3 and FGF8. *Curr. Biol.* **12**, 1117–1123.
35. Marin F. and Charnay P. (2000) Hindbrain patterning: FGFs regulate *Krox20* and *mafb/kr* expression in the otic/preotic region. *Development* **127**, 4925–4935.
36. Waskiewicz A. J., Rikhs H. A., and Moens C. B. (2002) Eliminating zebrafish PBX proteins reveals a hindbrain ground state. *Dev. Cell* **3**, 723–733.
37. Hertwig P. (1942) Sechs neue Mutationen bei der Hausmaus in ihrer Bedeutung für allgemeine Vererbungsfragen. *YX. Mensch. Vererbungslehre* **26**, 1–21.
38. Hertwig P. (1944) Die Genese der Hirn- und Gehörorganmißbildungen bei röntgenmutierten Kreisler-Mäusen. *Zeit. Konstlehere* **28**, 327–354.
39. Deol M. S. (1964) The abnormalities of the inner ear in *kreisler* mice. *J. Embryol. Exp. Morphol.* **12**, 475–490.
40. Manzanares M., Cordes S., Kwan C. T., Sham M. H., Barsh G. S., and Krumlauf R. (1997) Segmental regulation of *Hoxb3* by *kreisler*. *Nature* **387**, 191–195.
41. Manzanares M., Cordes S., Ariza-McNaughton L., Sadl V., Maruthinar K., Barsh G. S., and Krumlauf R. (1999) Conserved and distinct roles of *kreisler* in regulation of the paralogous *Hoxa3* and *Hoxb3* genes. *Development* **726(4)**, 759–769.
42. Wilkinson D. G., Bhatt S., Chavrier P., Bravo R., and Charnay P. (1989) Segment-specific expression of a zinc finger gene in the developing nervous system of the mouse. *Nature* **337**, 461–464.
43. Sham M. H., Vesque C., Nonchev S., et al. (1993) The zinc finger gene *Krox20* regulates *Hoxb-2* (*Hox 2.8*) during hindbrain segmentation. *Cell* **72(2)**, 183–196.
44. Nonchev S., Maconochie M., Vesque C., et al. (1996) The conserved role of *Krox20* in directing *Hox* gene expression during vertebrate hindbrain segmentation. *Proc. Natl. Acad. Sci. USA* **93(18)**, 9339–9345.
45. Giudicelli F., Taillebourg E., Charnay P., and Gilardi-Hebenstreit P. (2001) *Krox20* patterns the hindbrain through both cell-autonomous and non cell-autonomous mechanisms. *Genes Dev.* **15(5)**, 567–580.
46. Schneider-Maunoury S., Topilko P., Seitandou T., et al. (1993) Disruption of *Krox20* results in alteration of rhombomeres 3 and 5 in the developing hindbrain. *Cell* **75(6)**, 1199–1214.
47. Schneider-Maunoury S., Seitandou T., Charnay P., and Lumsden A. (1997) Segmental and neuronal architecture of the hindbrain of *Krox-20* mouse mutants. *Development* **124**, 1215–1226.
48. Swiatek P. J. and Gridley T. (1993) Perinatal lethality and defects in hindbrain development in *Krox20*^{-/-} mice for a targeted mutation of the zinc finger gene *Krox20*. *Genes Dev.* **7(11)**, 2071–2084.
49. Rovainen C. M. (1996) Feeding and breathing in lampreys. *Brain Behav. Evol.* **48(5)**, 297–305.
50. Wild J. M. (1993) The avian nucleus retroambiguus: a nucleus for breathing, singing and calling. *Brain Res.* **606**, 319–324.
51. Pack A. I. (1993) In: *Respiratory Control* (Speck, D. F., Dekin, M. S., Revelette, W. R. and Frazier, D. T., eds). Univ. Press of Kentucky, Lexington, pp. 52–57.
52. McLean H. A., Perry S. F., and Remmers J. E. (1995) Two regions in the isolated brainstem of the frog that modulate respiratory-related activity. *J. Comp. Physiol.* **177(2)**, 135–144.
53. Wilson R. J., Vasilakos K., Harris M. B., Straus C., and Remmers J. E. (2002) Evidence that ventilatory rhythmogenesis in the frog involves two distinct neuronal oscillators. *J. Physiol.* **540(2)**, 557–570.
54. Takeda R., Remmers J. E., Baker J. P., and Farber J. P. (1986) Postsynaptic potentials of bulbar respiratory neurons of the turtle. *Respir. Physiol.* **64**, 149–160.
55. Fortin G., Foutz A. S., and Champagnat J. (1994) Respiratory rhythm generation in chick hindbrain: effects of MK-801 and vagotomy. *NeuroReport* **5(9)**, 1137–1140.
56. Milsom W. K. (1991) Intermittent breathing in vertebrates. *Annu. Rev. Physiol.* **53**, 87–105.
57. Perry S. F., Wilson R. J., Straus C., Harris M. B., and Remmers J. E. (2001) Which came first, the lung or the breath? *Comp. Biochem. Physiol. A. Mol. Integr. Physiol.* **129(1)**, 37–47.
58. Bianchi A. L., Denavit-Saubié M., and Champagnat J. (1995) Central control of breathing in mammals: neuronal circuitry, membrane properties and neurotransmitters. *Physiol. Rev.* **75**, 1–45.

59. Richter D. W. and Spyer K. M. (2001) Studying rhythmogenesis of breathing: comparison of in vivo and in vitro models. *Trends Neurosci.* **24**(8), 464–472.
60. Suzue T. (1984) Respiratory rhythm generation in the in vitro brainstem-spinal cord preparation of the neonatal rat. *J. Physiol.* **354**, 173–183.
61. Smith J. C., Ellenberger H. H., Ballanyi K., Richter D. W., and Feldman J. L. (1991) Pre-Bötzinger complex: a region that may generate respiratory rhythm in mammals. *Science* **254**, 726–729.
62. Di Pasquale E., Monteau R., and Hilaire G. (1992) *In vitro* study of central respiratory-like activity of the fetal rat. *Exp. Brain Res.* **89**, 459–464.
63. Onimaru H. and Homma I. (1987) Respiratory rhythm generator neurons in medulla of brainstem-spinal cord preparation from newborn rat. *Brain Res.* **403**(2), 380–384.
64. Gray P. A., Rekling J. C., Bocchiaro C. M., and Feldman J. L. (1999) Modulation of respiratory frequency by peptidergic input to rhythmogenic neurons in the preBotzinger complex. *Science* **286**, 1566–1568.
65. Lieske S. P., Thoby-Brisson M., Telgkamp P., and Ramirez J. M. (2000) Reconfiguration of the neural network controlling multiple breathing patterns: eupnea, sighs and gasps. *Nat. Neurosci.* **3**(6), 600–607.
66. Borday V., Kato F., and Champagnat J. (1997) A ventral pontine pathway promotes rhythmic activity in the medulla of neonate mice. *NeuroReport* **8**, 3679–3683.
67. Onimaru H. and Homma I. (2003) A novel functional neuron group for respiratory rhythm generation in the ventral medulla. *J. Neurosci.* **23**(4), 1478–1486.
68. Denavit-Saubie M., Champagnat J., and Zieglansberger W. (1978) Effects of opiates and methionine-enkephalin on pontine and bulbar respiratory neurones of the cat. *Brain Res.* **155**(1), 55–67.
69. Morin-Surun M.-P., Boudinot E., Gacel G., Champagnat J., Roques B. P., and Denavit-Saubie M. (1984) Different effects of mu and delta opiate agonists on respiration. *Eur. J. Pharmacol.* **98**(2), 235–240.
70. Morin-Surun M.-P., Boudinot E., Dubois C., et al. (2001) Respiratory function in adult mice lacking the mu-opioid receptor: role of delta-receptors. *Eur. J. Neurosci.* **13**(9), 1703–1710.
71. Mellen N. M., Janczewski W. A., Bocchiaro C. M., and Feldman J. L. (2003) Opioid-induced quantal slowing reveals dual networks for respiratory rhythm generation. *Neuron* **37**(5), 821–826.
72. Morin-Surun M. P., Boudinot E., Kato F., Foutz A. S., and Denavit-Saubie M. (1995) Involvement of NMDA receptors in the respiratory phase transition is different in the adult guinea pig in vivo and in the isolated brainstem preparation. *J. Neurophysiol.* **74**, 770–778.
73. Blanco C. E. (1994) Maturation of fetal breathing activity. *Biol. Neonate* **65**, 182–188.
74. Jansen A. H. and Chernick V. (1983) Development of respiratory control. *Physiol. Rev.* **63**, 437–483.
75. Ramirez J. M., Quellmalz U. J., and Richter D. W. (1996) Postnatal changes in the mammalian respiratory network as revealed by the transverse brainstem slice of mice. *J. Physiol.* **491**, 799–812.
76. DeVries J. I. P., Visser G. H. A., and Precht H. F. R. (1982) The emergence of behavior. I. Qualitative aspects. *Early Hum. Dev.* **7**, 301–322.
77. Suzue T. (1994) Mouse fetuses in late gestation maintained *in vitro* by transplacental. *Neurosci. Res.* **21**, 173–176.
78. Greer J. J., Smith J. C., and Feldman J. (1992) Respiratory and locomotor patterns generated in the fetal rat brainstem-spinal cord *in vitro*. *J. Neurophysiol.* **67**, 996–999.
79. Fortin G., Champagnat J., and Lumsden A. (1994) Onset and maturation of branchiomotor activities in the chick hindbrain. *NeuroReport* **5**(9), 1149–1152.
80. Fortin G., Kato F., Lumsden A., and Champagnat J. (1995) Rhythm generation in the segmented hindbrain of chick embryos. *J. Physiol.* **486**(3), 735–744.
81. Clarke J. D. and Lumsden A. (1993) Segmental repetition of neuronal phenotype sets in the chick embryo hindbrain. *Development* **118**, 151–162.
82. Lumsden A., Clarke J. D. W., Keynes R., and Fraser S. (1994) Early phenotypic choices by neuronal precursors, revealed by clonal analysis of chick embryo hindbrain. *Development* **120**(6), 1581–1589.
83. Domínguez del Toro E., Borday V., Davenne M., Neun R., Rijli F. M., and Champagnat J. (2001) Generation of a novel functional neuronal circuit in *Hoxa1* mutant mice. *J. Neurosci.* **21**(15), 5637–5642.

84. Gavalas A., Trainor P., Ariza-McNaughton L., and Krumlauf R. (2001) Synergy between *Hoxa1* and *Hoxb1*: the relationship between arch patterning and the generation of cranial neural crest. *Development* **128**(15), 3017–3027.
85. Popperl H., Bienz M., Studer M., Chan S. K., Aparicio S., Brenner S., Mann R. S., and Krumlauf R. (1995) Segmental expression of *Hoxb-1* is controlled by a highly conserved autoregulatory loop dependent upon *exd/pbx*. *Cell* **81**(7), 1031–1042.
86. Di Rocco G., Mavilio F., and Zappavigna V. (1997) Functional dissection of a transcriptionally active, target-specific *Hox-Pbx* complex. *EMBO J.* **16**(12), 3644–3654.
87. Giudicelli F., Gilardi-Hebenstreit P., Mechta-Grigoriou F., Poquet C., and Charnay P. (2003) Novel activities of *Mafb* underlie its dual role in hindbrain segmentation and regional specification. *Dev. Biol.* **253**, 150–162.
88. Manzanares M., Trainor P. A., Nonchev S., et al. (1999) The role of *kreisler* in segmentation during hindbrain development. *Dev. Biol.* **211**, 220–237.
89. Voiculescu O., Taillebourg E., Pujades C., Kress C., Buart S., Charnay P., and Schneider-Maunoury S. (2001) Hindbrain patterning: *Krox20* couples segmentation and specification of regional identity. *Development* **128**, 4967–4978.
90. Chatonnet F., Domínguez del Toro E., Voiculescu O., Charnay P., and Champagnat J. (2002) Different respiratory control systems are affected in homozygous and heterozygous *kreisler* mutant mice. *Eur. J. Neurosci.* **15**, 684–692.
91. Lund J. P., Kolta A., Westberg K. G., and Scott G. (1998) Brainstem mechanisms underlying feeding behaviors. *Curr. Opin. Neurobiol.* **8**, 718–724.
92. Jacquin T. D., Borday V., Schneider-Maunoury S., Topilko P., Ghilini G., Kato F., Charnay P., and Champagnat J. (1996) Reorganisation of pontine rhythmogenic neuronal networks in *Krox-20* knockout mice. *Neuron* **17**, 747–758.
93. Fortin G., Jungbluth S., Lumsden A., and Champagnat J. (1999) Segmental specification of GABAergic inhibition during development of hindbrain neural networks. *Nat. Neurosci.* **2**, 873–877.
94. Abadie V., Champagnat J., and Fortin F. (2000) Branchiomotor activities in mouse embryo. *Neuroreport* **11**(1), 141–145.
95. Dawes G. S., Gardner W. N., Johnston B. M., and Walker D. W. (1983) Breathing in fetal lambs: the effect of brainstem section. *J. Physiol.* **335**, 535–553.
96. Hanson M. A. (1988) The importance of baro- and chemoreflexes in the control of the fetal cardiovascular system. *J. Dev. Physiol.* **10**(6), 491–511.
97. Kinney H. C., Filiano J. J., Sleeper L. A., Mandell F., Valdes-Dapena M., and Frost White W. (1995) Decreased muscarinic receptor binding in the arcuate nucleus in sudden infant death syndrome. *Science* **269**, 1446–1450.
98. Vert P., Aranda J. V., Catz C., and Yaffe S. (1994) Control of breathing during development, Apnea of the newborn, and in Sudden Infant Death Syndrome: In *Biol. Neonate* (J. P. Relier, ed.). Karger, Basel, Switzerland, pp. 133–280.
99. Cortez S. C. and Kinney H. C. (1996) Brainstem tegmental necrosis and olivary hypoplasia: a lethal entity associated with congenital apnea. *J. Neuropathol. Exp. Neurol.* **55**, 841–849.
100. Erickson J. T., Conover J. C., Borday V., Champagnat J., and Katz D. M. (1996) Mice lacking BDNF exhibit visceral sensory neuron losses distinct from mice lacking NT4 and display a severe developmental deficit in control of breathing. *J. Neurosci.* **16**, 5361–5371.
101. Gozal D. and Harper R. M. (1999) Novel insights into congenital central hypoventilation syndrome. *Curr. Opin. Pulm. Med.* **5**(6), 335–338.
102. Abadie V., Champagnat J., Fortin G., and Couly G. (1999) Sucking-deglutition-respiration and brain stem development genes. *Arch. Pediatr.* **6**, 1043–1047.
103. Lijowska A., Reed N., Chiodini B., and Thach B. (1995) Sequential reflex behavior leading to airway defense maneuvers and arousal from sleep in infants. *Respirat. Crit. Care Med.* **151**, A151.
104. Champagnat J. and Fortin G. (1996) Primordial respiratory-like rhythm generation in the vertebrate embryo. *TINS* **20**, 119–124.